JOURNAL OF MATERIALS SCIENCE 23 (1988) 2305–2309

Failure modes and fractographic study of glass–epoxy composite under dynamic compression

P. KUMAR, ANITA GARG*
*Department of Mechanical Engineering and *Department of Physics, Indian Institute of Technology, Kanpur 208016, India*

Unidirectional glass–epoxy composite has been tested under dynamic compressive loading conditions to study the different modes of failure and characterize them fractographically. Specimens of six fibre orientations θ = 0, 10, 30, 45, 60 and 90° with respect to the loading axis were loaded on Kolsky bars at an average strain rate of 265 sec^{-1}. The failure occurs on three different types of plane such that the fibre direction is preserved in all cases. Type A planes are tensile split planes and 0° specimens fail only in this mode. 10, 30 and 45° specimens shear on Type B planes by the combined action of normal and shear stresses. 60° and 90° specimens also fail by shear by the combined action of normal and shear stresses but on different types of planes called Type C planes. In these specimens the normal of the failure plane is found to make an angle lying between 55° and 70° with respect to the loading axis. The fractographs indicate intense matrix deformation and breaking up of fibre–matrix bonds for shear failure and comparatively clean fracture surfaces for tensile failure.

1. Introduction

Fibre-reinforced plastic (FRP) composites are becoming increasingly popular because of their wide applications. An interesting area to explore in this composite is the failure modes and the fractographic study of failed specimens.

At slow rates of loading, a uniaxial FRP indicates three kinds of failure modes in longitudinal compression: (i) fibre microbuckling, (ii) shear failure and (iii) interfacial failure or transverse splitting [1, 2]. Rosen [3] formulated the mechanism of failure in longitudinal compression through microbuckling of fibres in two different ways: out-of-plane buckling in the extensional mode and in-phase buckling in the shear mode. Experimental evidence of microbuckling was supplied by Rosen [3], Dow *et al.* [4] and Chou *et al.* [5]. However, the microbuckling theory is generally applicable to impractical composites with low fibre volume fractions. In the second type of failure mode, a broad band of shear damage is formed at an angle of 45° or greater to the fibres of a uniaxial specimen loaded in compression [6–9]. Sato *et al.* [10] studied the micromechanism of a shear band initiation. The failure begins with a fibre breakage which causes shear failure of matrix around the broken fibre tips. Further increase of the load leads to partial delamination and eventually a catastrophic crack propagation through the specimen. The third kind of compressive failure mode may be initiated by transverse splitting when the transverse tensile strain resulting from the Poisson's ratio effect exceeds the ultimate transverse capability of the composite [2, 11].

A unidirectional fibre composite subjected to transverse compressive loads generally fails by (i) shear failure of matrix or (ii) constituent debonding along with shear failure of the matrix [12, 13].

Relatively little work was been done to investigate the failure modes of fibre composites loaded in compression at high rates of loading [13–15]. In this paper, failure modes have been examined in a unidirectional glass–epoxy composite tested under dynamic compression. The dynamic testing has been conducted at an average strain rate of 265 sec^{-1} using the well-known Kolsky bars (split Hopkinson bar) technique [16–19] for six fibre orientations θ = 0, 10, 30, 45, 60 and 90° with respect to the loading axis. The characteristic features of the failed surfaces as seen through the scanning electron microscope (SEM) are also presented.

2. Experimental details

2.1. Kolsky pressure bars technique

The Kolsky pressure bars technique is a standard and well-developed technique [16–19] for studying the dynamic behaviour of materials. In this technique, a short cylindrical specimen is sandwiched between two long elastic pressure bars of circular cross-section. The bars, known as incident and transmitted, were fabricated from hardened EN-24 steel which remained elastic during the test. The diameter of each bar was 19 mm. A stress pulse was generated in the incident bar by impacting it with a striker which was accelerated in an air-gun of 19 mm bore. The amplitude of the incident pulse was varied from 150 to 530 MPa and its duration from 115 to 195 μsec. On reaching the specimen, a part of the incident pulse was reflected

0022–2461/88 $03.00 + .12

and the rest was transmitted. The incident, reflected and transmitted pulses were recorded on a dual-beam Nicolet digital oscilloscope through strain gauges mounted on the pressure bars. The state of stress in the specimen was calculated from the recorded pulses using the one-dimensional theory of elastic wave propagation [20].

2.2. Specimen preparation

Unidirectional plates of thickness 21 mm were fabricated in the laboratory by a filament winding technique. E-glass fibres (obtained from FGP, India) and epoxy resin (Araldite CY 230 obtained from Ciba, India) were used as the reinforcement and the matrix material, respectively. The fibre volume fraction of the plates as determined by a burn test was 46%. Cylindrical specimens were machined from the fabricated plate such that the fibres were parallel and normal to the loading axis for longitudinal (θ = 0°) and transverse (θ = 90°) specimens. Off-axis specimens were machined such that the fibres were oriented at angles 10, 30, 45 and 60° with their geometric axis. The end-faces of each specimen were made flat and smooth by polishing. At least four specimens were tested for each orientation.

After loading the specimens on the Kolsky set-up, the fractured specimens were examined under SEM. For this purpose the surfaces were made conducting by coating them with a thin layer of gold.

3. Results and discussion

3.1. Stress–strain behaviour

The dynamic stress–strain curves at an average strain rate of 265 sec^{-1} are plotted in Fig. 1. The stress–strain curves for 0° and 10° specimens exhibit moduli comparable to the modulus of a theoretical curve for 0° uniaxial glass fibre reinforced plastic (GFRP). The theoretical curve is evaluated through the Rule of Mixtures using the quasistatic properties of glass fibre and epoxy. The curves for 30, 45, 60 and 90° specimens lie in a narrow band extending over the low stress–high strain region. They are distinctly separated from the curves for 0 and 10° and lie close to the theoretical curve for a 90° specimen obtained through the approach of the Rule of Mixtures (constant stress model).

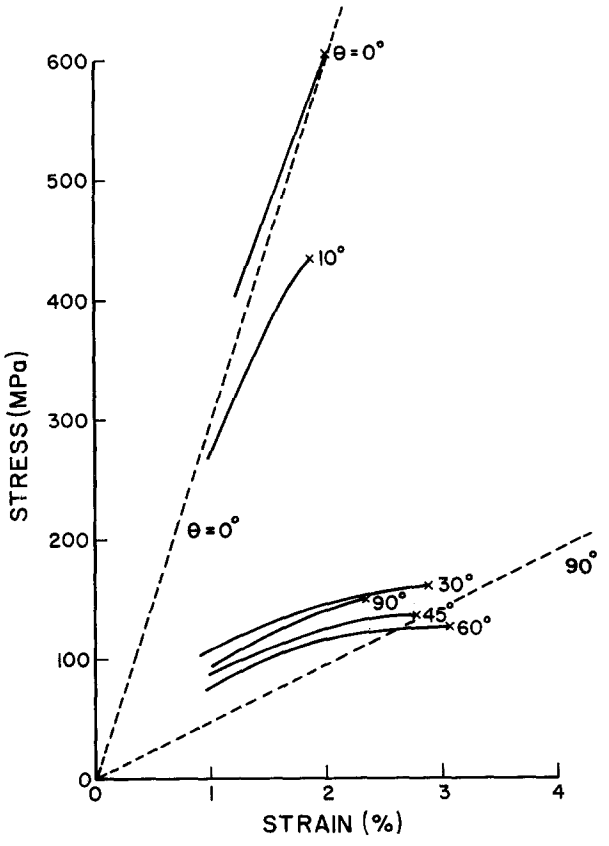

Figure 1 (——) Dynamic ($\dot{\varepsilon}$ = 265 sec^{-1}) stress–strain curves for various fibre orientations θ, and (– – –) theoretically predicted curves for 0 and 90° fibre orientations.

3.2. Modes of failure

The fracture always occurs such that the failure plane is parallel to the fibres. The fracture propagates along three types of plane labelled as Types A, B and C in Fig. 2a. Type A exhibits planes of tensile failure. In this mode of failure, the compressive loading causes transverse tensile strain because of Poisson's ratio, and as the tensile strain exceeds the ultimate strain in the transverse direction failure occurs by tensile splitting. Cracks running through the specimen parallel to the loading axis are the characteristic feature of this mode. Longitudinal specimens (θ = 0°) fracture only in this mode and the fractured pieces generally do not separate. White strips indicating fracture run from top to bottom of the specimen (Fig. 3). Furthermore, the specimens under dynamic compression are not found to fail in the shear mode, a prominent mode of failure at a quasistatic rate of loading [6–9].

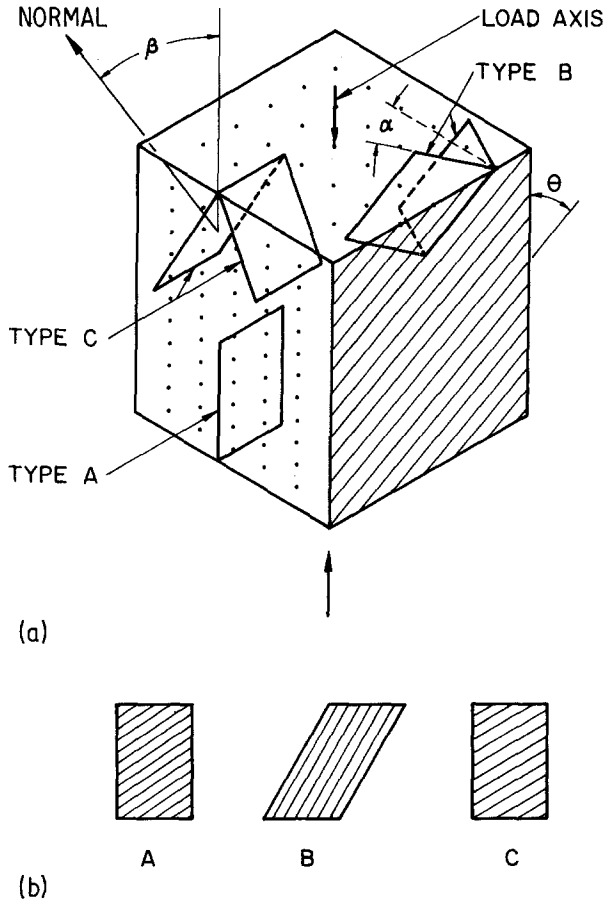

Figure 2 (a) Type A, B and C planes; (b) the fibre orientations on failure surfaces.

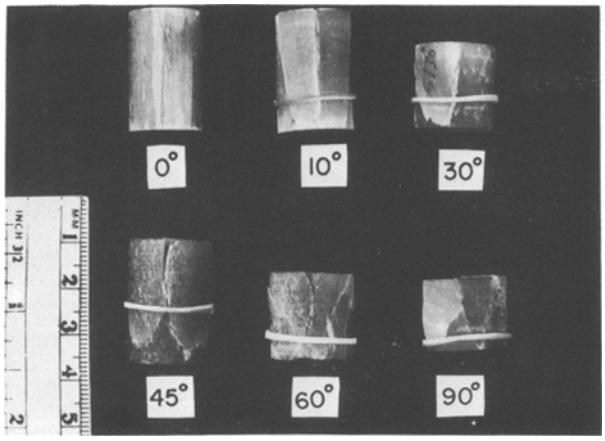

Figure 3 Specimens showing tensile cracks.

Tensile cracks have been observed on the surfaces of off-axis specimens also. In a 10° specimen, the tensile crack runs from top to bottom in addition to other types of crack. But in 30, 45, 60 and 90° specimens the tensile crack runs only through a short distance before it branches into other cracks producing Type B and C failure planes. This indicates that the predominant mode of failure in these specimens is not tensile splitting.

Type B failure planes are produced by shear failure. The fracture propagates along the fibres, i.e. the failure occurs at the fibre angle θ with the loading axis. This mode of failure is commonly observed in specimens of 10, 30 and 45° fibre orientation as shown in Fig. 4. In off-axis specimens, for an applied stress σ the shear component along the fibres, τ_{LT}, and the normal component, σ_n, are given by

$$\tau_{LT} = \sigma \sin\theta \cos\theta$$

$$\sigma_n = \sigma \sin^2\theta$$

Values of τ_{LT}/σ and σ_n/σ for different fibre orientations θ are tabulated in Table I. For 10, 30 and 45° specimens the normal component of the compressive stress is small compared to that of 60° and 90° specimens and is also less than (or equal to for 45° specimens) its corresponding shear component. Hence these specimens are susceptible to easy fracture by shear along the fibres.

TABLE I Shear and normal components of the compressive stress, σ, for various fibre orientations

Stress	θ (deg)					
	0	10	30	45	60	90
Shear τ_{LT}/σ	0	0.17	0.43	0.50	0.43	0
Normal σ_n/σ	0	0.03	0.25	0.50	0.75	1

The fractured surfaces of 10, 30 and 45° specimens are shown in Fig. 5. The surfaces are identical to the Type B plane shown in Fig. 2b, where fibres are not perpendicular to the edges corresponding to the end-faces. The fracture surface in general makes an angle α, shown for clarity in Fig. 2a, with the plane perpendicular to the tensile split plane containing the loading axis. An extreme case of Type B plane is the Type A plane when α becomes 90°. Hence Type B planes are defined by the two angles θ and α shown in Fig. 2a. α is found to lie within 12 and 24° for $\theta = 10°$, 20 to 31° for $\theta = 30°$ and 27 to 37° for $\theta = 45°$ specimens.

For a general value of α, τ_{LT} and σ_n are given by

$$\tau_{LT} = \frac{\sigma \sin\theta}{(1 + \tan^2\theta + \tan^2\alpha)^{1/2}}$$

$$\sigma_n = \frac{\sigma \tan^2\theta}{1 + \tan^2\theta + \tan^2\alpha}$$

The variations of τ_{LT}/σ and σ_n/σ with α for $\theta = 10$, 30 and 45° are plotted in Fig. 6. As the angle α increases, both τ_{LT}/σ and σ_n/σ begin to decrease but the decrease in σ_n/σ is faster than that of τ_{LT}/σ. Thus in Type B planes, failure occurs at the angle θ and proceeds along that particular value of α where the shear stress is such that it facilitates shear failure by the reduction in normal compressive stress. Fracture in 10, 30 and 45° specimens are found to occur on planes where the decrease in σ_n/σ is almost double the decrease in τ_{LT}/σ from the $\alpha = 0°$ value.

The sheared faces of Type B planes are not smooth but exhibit hills and valleys which are most prominent for 45° specimens.

For θ greater than 45°, the normal component of the compressive stress is larger than the corresponding shear component and therefore it tends to suppress the shear failure on Type B planes. Hence in 60° and 90° specimens failure occurs on a different set of planes labelled as Type C in Fig. 2a. Under the combined

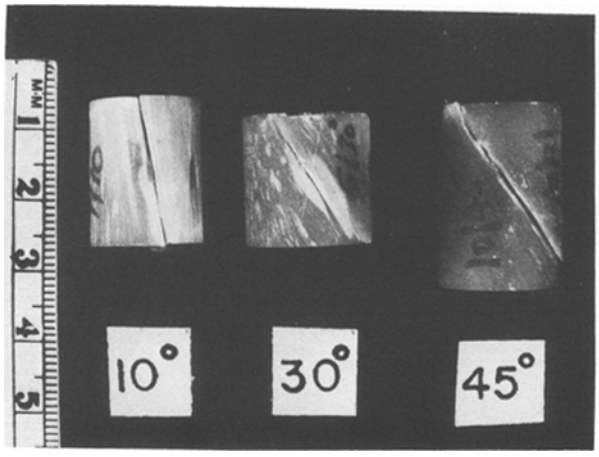

Figure 4 Crack along fibres in 10, 30 and 45° specimens.

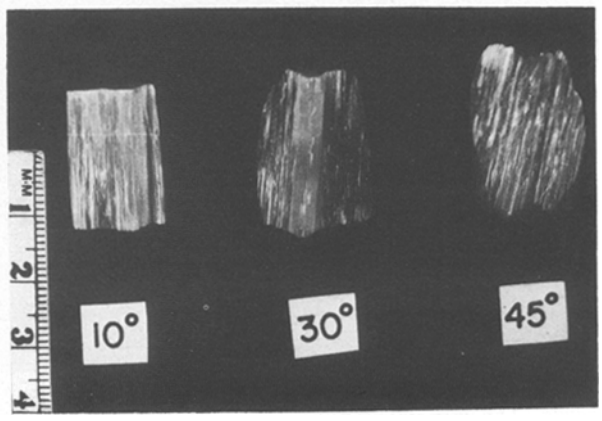

Figure 5 Failed surfaces of 10, 30 and 45° specimens.

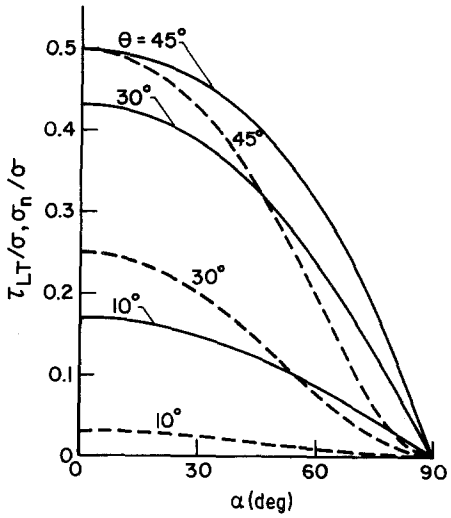

Figure 6 Variation of (——) shear (τ_{LT}/σ) and (– – –) normal (σ_n/σ) components of stress with angle α.

action of normal and shear stresses, failure occurs on that particular Type C plane where the combination of shear and normal compressive stress satisfies the failure criterion. The fractured specimens of 60 and 90° fibre orientation are shown in Fig. 7 and their failed surfaces in Fig. 8. The normal to the fracture planes in both of these specimens is found to make an angle β (shown in Fig. 2a) lying between 55 and 70° with the loading axis. This agrees closely with the study of Collings [12], who has studied the static transverse behaviour of carbon-fibre reinforced plastic and found this angle to be 60°.

3.3. Fractured surfaces

Since the fractured pieces of 0° specimens do not separate, it has not been possible to examine them under SEM. However, the tensile split plane, Type A, of a $\theta = 45°$ specimen as seen through SEM is shown in Fig. 9. The fractograph shows very few pieces of matrix sticking to the fibres and not much matrix deformation. This suggests that the splitting occurs by debonding at the fibre–matrix interface, leaving the fracture surface rather clean.

The fracture surfaces of 10° and 45° specimens are shown in Figs 10 and 11, respectively. These micrographs show shear deformation in planes of Type B. Both the fractographs depict extensive surface damage.

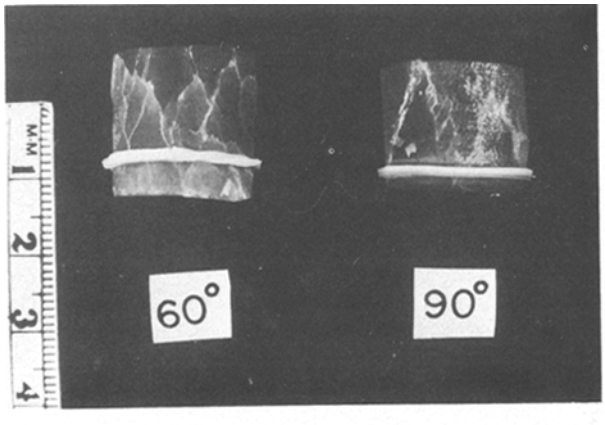

Figure 7 Fractured specimens showing cracks on the surfaces of 60 and 90° specimens.

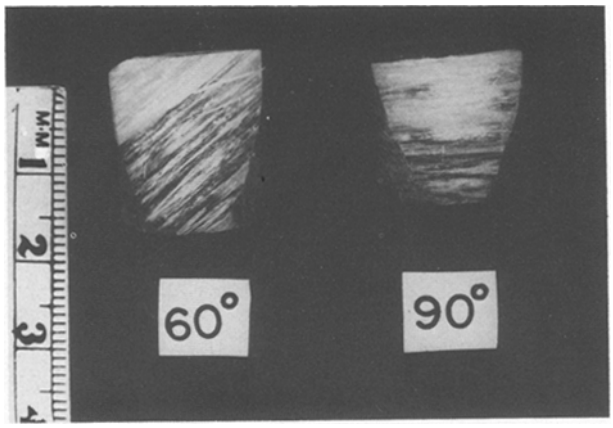

Figure 8 Failed surfaces of 60 and 90° specimens.

Large number of small pieces of broken epoxy, varying in size from 1 to 15 μm, can be seen sticking to the failed surface. A noticeable feature of the fractographs is the intense deformation of the matrix. Dual branched microcracks emanating in the matrix material from both sides of the binding fibres (Fig. 10) are clearly visible. Such cracks may be attributed to the interfacial stresses created due to differences in the elastic properties of the fibres and the matrix. As the deformation increases, the stresses increase, and microcracks coalesce leading to failure [13]. Another noticeable characteristic is the peculiar pattern in which the matrix deforms (Fig. 11). Sutton [21] has observed such deformation patterns in unreinforced epoxy resin and called them "hackles". Thus, in Type B planes, fracture occurs by the breaking up of fibre–matrix bonds which leaves behind large number of epoxy pieces, and by the intense matrix deformation which occurs by the formation of dual branched microcracks and hackles.

A fractograph of a 60° specimen depicting deformation on Type C planes is shown in Fig. 12. As compared to the fractographs of Type B planes, this fractograph is quite clean. Hardly any pieces of broken matrix stick to the fibres, but matrix deformation in the form of hackle formation is very distinctly visible in this micrograph also. A mechanism of hackle formation based on the initiation of matrix cracks near a fibre–matrix boundary has been proposed by Morris [15] and experimental evidence for it was provided by Kline and Chang [13] from a graphite–epoxy composite tested under static tension. More

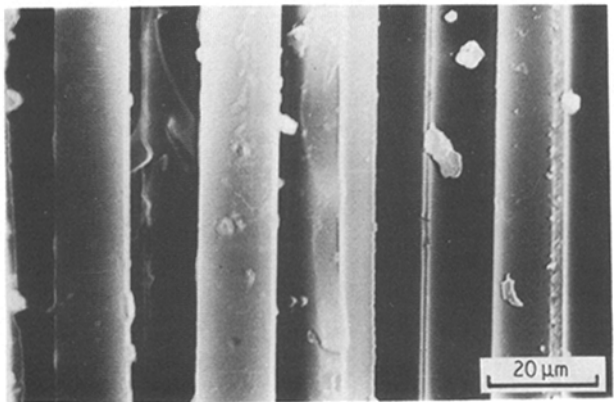

Figure 9 Fractograph of a tensile split plane in 45° specimen.

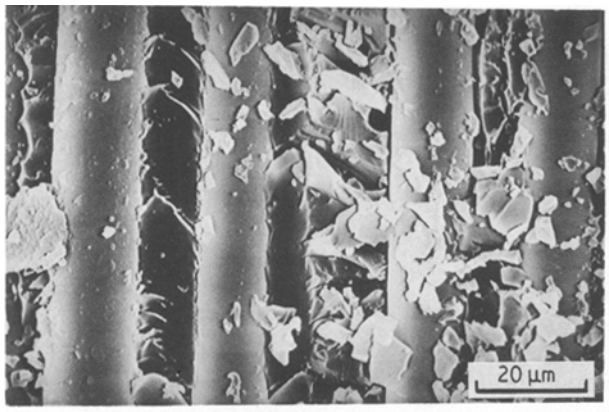

Figure 10 Fractograph of a shear split plane (Type B) in 10° specimen.

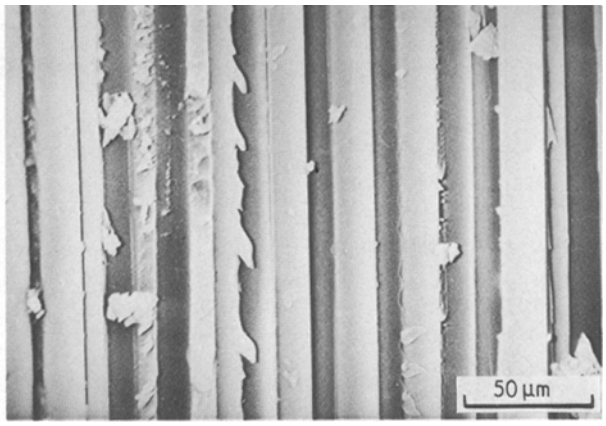

Figure 12 Fractograph of a shear split plane (Type C) in 60° specimen.

evidence is provided here from the glass–epoxy composite tested under dynamic compressive loading conditions.

4. Conclusions

The stress–strain behaviour in compression of unidirectional glass–epoxy composite has been determined at an average strain rate of 265 sec^{-1} for six fibre orientations, 0, 10, 30, 45, 60 and 90°.

The failure occurs on three types of plane such that the fibre direction is preserved in all orientations. 0° specimens fail on Type A planes by tensile splitting. Off-axis specimens fail by shear by the combined action of normal and shear stresses. In 10, 30 and 45° specimens, failure occurs along the fibres on Type B planes where the reduction in normal compressive stress facilitates shear failure. In 60° and 90° specimens, failure also occurs by shear but on Type C planes which are parallel to the fibres, but whose normal makes an angle lying between 55 and 70° with the loading axis.

SEM fractographs indicate very little surface damage for tensile split (Type A) planes. Shear failure planes (Types B and C) exhibit a large amount of matrix deformation in the form of hackle formation and dual branched microcracks. Type B planes also exhibit severe breaking up of fibre–matrix bonds.

Acknowledgements

The authors deeply appreciate the valuable suggestions provided by Professor B. D. Agarwal in carrying out this work. They are also indebted to the Aeronautics Research and Development Board (Structures Panel), the Government of India, for sponsoring the work. The authors would like to thank Professor K. Rajaiah of ADE Bangalore, Dr K. N. Raju of NAL Bangalore and Professor N. S. Venkataraman of MIT Madras for their help and encouragement.

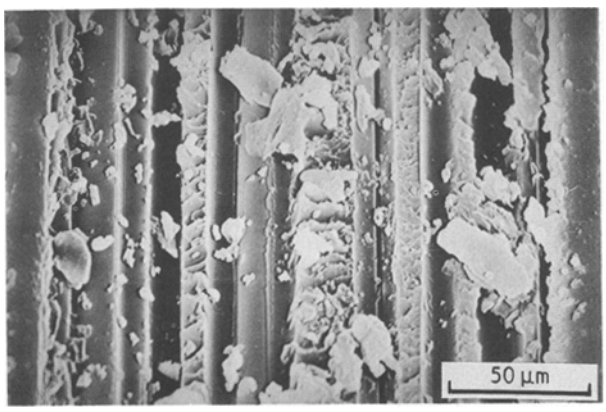

Figure 11 Fractograph of a shear split plane (Type B) in 45° specimen.

References

1. T. W. CHOU and A. KELLY, *J. Mater. Sci.* **15** (1980) 327.
2. B. D. AGARWAL and L. J. BROUTMAN, "Analysis and Performance of Fibre Composites" (Wiley, New York, 1980) p. 48.
3. B. W. ROSEN, in "Fibre Composite Materials" (American Society for Metals, Cleveland, Ohio, 1965) p. 37.
4. N. F. DOW, B. W. ROSEN and Z. HASHIN, "Studies of Mechanics of Filament Composites", NASA Report No. CR-492 (1966).
5. T. W. CHOU, R. L. McCULLOUGH and R. B. PIPES, *Sci. Amer.* **254** (October, 1986) 193.
6. E. M. De FERRAN and B. HARRIS, *J. Compos. Mater.* **4** (1970) 62.
7. R. L. SIERAKOWSKI, G. E. NEVILL, C. A. ROSS and E. R. JONES, *ibid.* **5** (1971) 362.
8. N. L. HANCOX, *J. Mater. Sci.* **10** (1975) 234.
9. M. R. PIGGOT and P. WILDE, *ibid.* **15** (1980) 2811.
10. N. SATO, T. KURAUCHI and O. KAMIGAITO, *ibid.* **21** (1986) 1005.
11. L. B. GRESZEZUCK, in Proceedings of AIAA/ASME/SAE 15th Structure, Structural Dynamics and Materials Conference, April 1974.
12. T. A. COLLINGS, *Composites* **5** (May 1974) 108.
13. R. A. KLINE and F. H. CHANG, *J. Compos. Mater.* **14** (1980) 315.
14. O. ISHAI, A. E. MOCHLENPAH and A. PREIS, *J. Eng. Mech. Div., Proc. Amer. Soc. Civil Engrs* **96** (5) (1970) 739.
15. G. MORRIS, paper presented at ASTM Symposium on Composite Materials, Philadelphia, 1978.
16. H. KOLSKY, *Proc. Phys. Soc. B* **62** (1949) 676.
17. E. D. H. DAVIES and S. C. HUNTER, *J. Mech. Phys. Solids* **11** (1963) 155.
18. U. S. LINDHOLM, *ibid.* **12** (1964) 317.
19. W. E. JAHSMAN, *J. Appl. Mech.* **38** *Trans. ASME* **93** *Ser. E* (1971) 75.
20. J. D. ACHEANBACH, in "Wave Propagation in Elastic Solids" (North-Holland, Amsterdam, 1973) p. 21.
21. S. SUTTON, *Eng. Fract. Mech.* **6** (3) (1974) 581.

Received 7 October 1986
and accepted 15 July 1987